Phosphoinositide-3-kinase-independent contractile activities associated with Fcγ-receptor-mediated phagocytosis and macropinocytosis in macrophages

Nobukazu Araki[1],*, Tanenori Hatae[1], Aizo Furukawa[2] and Joel A. Swanson[3]

[1]Department of Histology and Cell Biology, Kagawa Medical University, Miki, Kagawa 761-0793, Japan
[2]Department of Biochemistry, Kagawa Medical University, Miki, Kagawa 761-0793, Japan
[3]Department of Microbiology and Immunology, University of Michigan Medical School, Ann Arbor, MI 48109-0620, USA
*Author for correspondence (e-mail: naraki@kms.ac.jp)

Summary

Previous studies have shown that Fcγ receptor (FcR)-mediated phagocytosis and macropinocytosis in macrophages consist of two dissociable activities: a phosphoinositide 3-kinase (PI3K)-independent extension of phagocytic cups and a PI3K-dependent contractile mechanism that closes phagosomes and ruffles into intracellular organelles. Here, we identify an additional contractile activity that persists in the presence of the PI3K inhibitor wortmannin. ML-7, an inhibitor of myosin-light-chain kinase (MLCK), inhibited FcR-mediated phagocytosis, macropinocytosis and cell movements associated with ruffling. Scanning electron microscopy demonstrated a striking difference in morphology between phagocytic cups in the different inhibitors: whereas phagocytic cups of control cells and wortmannin-treated cells conformed closely to particles and appeared to have constricted them, the phagocytic cups in cells treated with ML-7 were more open. Video microscopy of macrophages expressing green-fluorescent-protein (GFP)–actin fusions revealed that bound IgG-opsonized erythrocytes were squeezed during phagosome formation and closure. In ML-7, GFP–actin-rich protrusions extended outward but failed to squeeze particles. Moreover, in contrast to the effects of PI3K inhibitors, ML-7 markedly reduced ruffle movement, and perturbed circular ruffle formation. These PI3K-independent myosin-II-based contractile activities that squeeze phagocytic cups and curve ruffles therefore represent a third component activity of the actin cytoskeleton during phagocytosis and macropinocytosis.

Movies available online

Key words: Myosin, Myosin light chain kinase, Actin, Phosphoinositide 3-kinase, Phagocytosis, Macropinocytosis

Introduction

Phagocytosis and macropinocytosis are essential components of innate immunity. Most conspicuous in macrophages, dendritic cells and cellular slime molds, these activities consist of circular protrusion (phagocytic cup or ruffle extension) and closure to take up extracellular particles or fluid. Such cell-surface motilities are highly dependent on actin polymerization and reorganization, and involve a variety of actin-binding proteins and myosins (Stendahl et al., 1980; Swanson and Baer, 1995; Allen and Aderem, 1996a; Aderem and Underhill, 1999; Swanson et al., 1999; Araki et al., 2000; Diakonova et al., 2002). Although the signaling pathway for F-actin polymerization during phagocytosis and macropinocytosis has been extensively studied (for reviews see Allen and Aderem, 1996a; Kwiatkowska and Sobota, 1999; Lennartz, 1999; Greenberg, 2001; May and Machesky, 2001), the mechanics of phagosome and macropinosome formation remain less well defined.

In Fcγ receptor (FcR)-mediated phagocytosis, phagocytic cup extension along the surfaces of immunoglobulin G (IgG)-opsonized particles is mediated by the sequential interactions between IgG Fc regions and FcR, in a process referred to as the zipper closure model (Greenberg and Silverstein, 1993).

Recent studies have indicated that the zipper closure model is insufficient to explain phagocytosis. Phosphoinositide 3-kinase (PI3K) inhibitors such as wortmannin and LY294002 inhibit the closure of phagosomes, but not phagocytic cup formation along IgG-opsonized particles (Araki et al., 1996), indicating that closure of phagocytic cups into phagosomes requires additional mechanisms that employ PI3K. Cox et al. (Cox et al., 1999) pointed out the importance of PI3K-dependent vesicle transport for maximal phagocytic cup extension during phagocytosis of large particles. Furthermore, several events in phagocytosis seem to lie downstream of PI3K (Gold et al., 1999; Didichenko et al., 2000; Vieira et al., 2001; Cox et al., 2002).

The myosin family of actin-based mechanochemical motors is an important component of the phagocytic apparatus. Myosins I, II, V, IX and X have been localized to macrophage phagosomes at various stages of their formation (Stendahl et al., 1980; Allen and Aderem, 1995; Swanson et al., 1999; Al-Haddad et al., 2001; Cox et al., 2002; Diakonova et al., 2002; Olazabal et al., 2002), suggesting that they play distinct roles in phagocytosis. Morphological studies identified a PI3K-dependent contractile activity, capable of constricting deformable erythrocytes caught between two macrophages

(Swanson et al., 1999). Myosin IC localized to the distal margin of phagocytic cups, suggesting that it mediated a PI3K-dependent, purse-string-like contractile activity that closed the cup aperture into an intracytoplasmic phagosome (Swanson et al., 1999). Consistent with this model, Cox et al. (Cox et al., 2002) identified a role for myosin X in phagocytosis, which is notable because myosin X contains a pleckstrin-homology domain that recognizes phosphatidylinositol(3,4,5)triphosphate. Although myosin II (known as conventional myosin) has been localized around forming phagosomes (Stendahl et al., 1980; Swanson et al., 1999; Diakonova et al., 2002), its precise role and regulation in phagocytosis remain to be elucidated. One aim of this study is to elucidate the role of myosin II in the process of phagocytosis and to clarify the relationship of myosin function to PI3K signaling.

Macropinocytosis is a form of fluid-phase endocytosis that provides an efficient route for non-selective uptake of extracellular solute macromolecules (Swanson and Watts, 1995). Recent attention has been directed toward the mechanism of macropinocytosis, because that route is used for MHC class I and class II antigen presentation in dendritic cells and macrophages (Norbury et al., 1995; Sallusto et al., 1995; Nobes and Marsh, 2000). Unlike micropinocytosis mediated by clathrin-coated vesicles and small uncoated vesicles (~100 nm diameter), macropinocytosis is associated with active cell-surface ruffling. Macropinosomes (0.5-5 μm diameter) arise from the deformation of ruffles, which are actin-rich cell-surface protrusions. Circular ruffles, formed by inward curving of peripheral ruffles, are considered to be precursors of macropinosomes, in that they often close into macropinosomes.

There are many similarities in the signaling for macropinocytosis and FcR-mediated phagocytosis. Like FcR-mediated phagocytosis, macropinocytosis involves Rac1, Cdc42 and Arf6 (Radhakrishna et al., 1996; Zhang et al., 1999; Nobes and Marsh, 2000; West et al., 2000), and the closure of cup-shaped circular ruffles into macropinosomes requires PI3K activity (Araki et al., 1996). However, some differences in their signaling, regulation and mechanism are notable (Swanson and Baer, 1995; Swanson and Watts, 1995; Niewohner et al., 1997). For example, unlike phagocytosis, the cell-surface protrusions forming circular ruffles can form without the guidance of any particle surface. Therefore, one might expect that shaping ruffles into macropinosomes would require spatial and temporal controls distinct from those for phagocytic cup formation. Although myosin II has been shown to generate force for cell movements, its role in macropinocytosis is not clear. It is of interest to determine whether myosin II contributes similarly to macropinocytosis and phagocytosis.

ML-7 is an inhibitor of MLCK (Saitoh et al., 1987), and inhibition of MLCK results in selective perturbation of myosin II function (Somlyo and Somlyo, 1994; Ruchhoeft and Harris, 1997). Although higher concentrations of ML-7 might inhibit other protein kinases, the concentration of ML-7 we used does not much affect other protein kinases (Mansfield et al., 2000). In the present study, we have compared the effects of the MLCK inhibitor and inhibitors of PI3K on macropinocytosis and phagocytosis. We describe a novel actomyosin-driven motion that squeezes phagocytic cups and promotes circular-ruffle formation for macropinocytosis. This now distinguishes a third activity of the actin cytoskeleton in phagocytosis.

Materials and Methods

Reagents and cells

Dulbecco's modified essential medium (DME) and fetal bovine serum (FBS) were from Gibco BRL (Grand Island, NY). Wortmannin, bovine serum albumin (BSA) and fluorescein-dextran M_r 150×10^3 (FDx150) were from Sigma Chemical (St Louis, MO). ML-7 was from BIOMOL Research Labs (Plymouth Meeting, PA). LY294002 was from Calbiochem (La Jolla, CA). Human recombinant macrophage colony stimulating factor (M-CSF) was from R&D Systems (Minneapolis, MN). All other reagents were purchased from Wako Pure Chemical (Osaka, Japan) unless otherwise indicated.

Bone-marrow-derived macrophages were obtained from femurs of C3H HeJ mice as previously described (Araki et al., 1996). After 6 or 7 days of culture, macrophages were harvested from dishes and plated onto coverslips or 24-well dishes, then incubated overnight in DME-10F (DME with 10% heat-inactivated FBS). 30 minutes before experiments, DME-10F was replaced with Ringer's buffer (RB) consisting of 155 mM NaCl, 5 mM KCl, 1 mM MgCl$_2$, 2 mM Na$_2$HPO$_4$, 10 mM glucose, 10 mM Hepes pH 7.2 and 0.5 mg ml^{-1} BSA. These bone-marrow-derived macrophages were used for all but the transfection experiments.

For transfection with an enhanced GFP (EGFP)-fused actin expression plasmid (pEGFP-actin, CLONTECH, Palo Alto, CA), macrophage-like RAW264.1 cells, obtained from Riken Cell Bank (Tsukuba, Japan), were plated onto 25 mm circular coverslips in 35 mm dishes filled with DME-10F. The pEGFP-actin was transfected into the cells using a DNA transfection reagent, TransFast (Promega, Madison, WI). Fluorescence was observed by video microscopy 48 hours after transfection, as described below.

Phagocytosis and microscopy

For phagocytosis, sheep erythrocytes were opsonized with rabbit anti-sheep erythrocyte IgG (1:200 dilution, Organon Teknika-Cappel) and resuspended in PBS at 10^9 erythrocytes ml^{-1}. 10 μl of a suspension of IgG-opsonized sheep erythrocytes (IgG-Es) was added to each 24-well dish containing macrophages on 12 mm circular coverslips. Macrophages were then incubated for various times at 37°C, to allow phagocytosis. For quantitative assay of phagocytosis, after a 30-minute incubation with IgG-Es, cells on coverslips were dipped into distilled water for 30 seconds to disrupt extracellularly exposed IgG-Es by low osmolarity, then fixed with 4% paraformaldehyde in a buffer. For the binding assay, cells were incubated with IgG-Es for 30 minutes at 4°C, briefly washed in cold PBS to remove unbound IgG-Es and fixed. The number of IgG-Es in 100 macrophages was counted under a phase-contrast microscope and the number of bound or internalized IgG-Es per macrophage was expressed as the binding or phagocytic index, respectively.

For fluorescence microscopy of phagocytosis combined with filamentous actin (F-actin) staining, cells were fixed for 30 minutes at room temperature with 4% paraformaldehyde and 0.1% glutaraldehyde in 100 mM phosphate buffer, pH 7.4, containing 6.8% sucrose (PB/sucrose). To distinguish extracellularly exposed IgG-Es from intraphagosomal IgG-Es, macrophages were incubated with FITC-labeled anti-rabbit IgG (1:50 dilution in PBS), which was not accessible to intraphagosomal IgG-Es, for 15 minutes at room temperature. Then, F-actin was stained with rhodamine phalloidin (Molecular Probe, 5 unit ml^{-1} PBS containing 0.25% Triton X-100).

For immunocytochemistry, cells on 12-mm coverslips were fixed with 4% paraformaldehyde in PB/sucrose for 30 minutes, rinsed in PBS, and permeabilized with 0.25% Triton X-100 in PBS followed by treatment with a blocking buffer (0.5% BSA, 0.2% gelatin, 0.25% Triton X-100 in PBS). Then, cells were incubated with rabbit polyclonal anti-myosin-II antibody (1:100 dilution; Biomedical Technologies, Stoughton, MA) or goat polyclonal anti-phospho-myosin-light-chain (P-MLC) antibody (1:100 dilution; Santa Cruz Biotechnology) for 90 minutes at room temperature. After rinsing in

PBS, cells were labeled with FITC-anti-rabbit IgG and/or Texas-red anti-goat IgG (Vector, Burlingame, CA).

Coverslips were mounted on glass slides using a FluoroGuard (BioRad) and observed with an epifluorescence microscope (Nikon TE 300) operated by MetaMorph Imaging System (Universal Imaging, West Chester, PA).

For scanning electron microscopy (SEM) of phagocytosis, macrophages on small coverslips were fixed with 2% glutaraldehyde in PB/sucrose for 1 hour at room temperature. Coverslips were then rinsed in a buffer, post-fixed with 1% osmium tetroxide, treated with 1% tannic acid, conventionally processed for SEM and observed by a Hitachi S-900 SEM as previously described (Araki et al., 1996).

Spectrofluorometric assay of macropinocytosis

Macropinocytosis was stimulated by the addition of human recombinant M-CSF (2000 unit ml^{-1}) to the macrophage culture (Racoosin and Swanson, 1992; Araki et al., 1996).

After 30-minute incubation with 1.0 mg ml^{-1} FDx150 to allow fluid-phase pinocytosis, dishes were drained and rinsed twice in 1 l PBS plus 1 mg ml^{-1} BSA and then once in 1 l PBS, each at 4°C for 5 minutes. Cells were lysed in a lysis buffer consisting of 0.1% Triton X-100 and 50 mM Tris pH 8.5. The amount of fluorescence in cell lysates was measured by a spectrofluorometer (Hitachi 650-40) and normalized by the total cell protein.

Video microscopy and digital image analysis

Macrophages were plated onto 25 mm circular coverslips in 35 mm culture dishes. The culture medium was replaced with RB 1 hour before experiments. The coverslip was assembled into a stainless steel cell chamber (Atto Instruments, Rockville, MD) and placed in a temperature-controlled stage at 37°C on an inverted microscope (Nikon TE300). Living cells were observed using a 100 lens with phase-contrast optics. Before and after addition of drugs, time-lapse video images were collected using a cooled CCD camera (IFG-300, Dage-MTI, Michigan City, IN) and MetaMorph Imaging System. These images were revealed as 8-bit digital images consisting of pixels with 256 shades of gray (0-255 gray value). Time-lapse video microscopic images taken at a 10-second interval using MetaMorph were assembled to QuickTime movies. Videos accompany Fig. 4A,B, Fig. 7A-D and are available in the online version at http://jcs.biologists.org/supplemental.

Ruffling activity was quantified using a subtraction-based image analysis developed with MetaMorph software (Araki et al., 1996). In phase-contrast images of living cells, ruffles were seen as phase-dense bands that grew in length and migrated centripetally along the upper surface of the cells. Using 20-second interval time-lapse series, one frame of an image was subtracted, pixel by pixel, from the frame taken 20 seconds later. A gray value of 120 was then added to all pixels of the subtracted image. Change of phase density in a 20-second interval produced contrast in the subtracted image. The average of standard deviations of gray values in the cell region of 10 subtracted images was calculated as the ruffling activity index.

Results

Myosin inhibition perturbs phagocytosis as well was PI3K inhibition

We quantified the effects of various inhibitors of PI3K, MLCK or F-actin on phagocytosis of IgG-Es by bone-marrow-derived macrophages. As previously reported (Araki et al., 1996), the PI3K inhibitors LY294002 and wortmannin markedly reduced the number of IgG-Es internalized into fully closed phagosomes. A MLCK inhibitor (10-20 µM ML-7) reduced the number of intracellular IgG-Es in a dose-dependent manner,
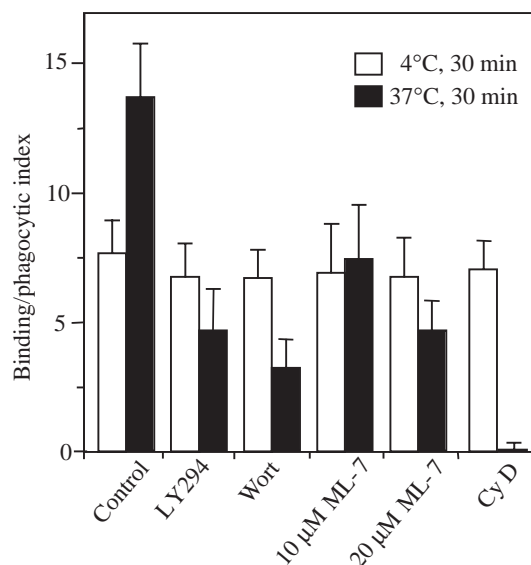

Fig. 1. Effects of various inhibitors for PI3K, MLCK and F-actin on binding and phagocytosis of IgG-Es. Macrophages were fed IgG-Es in RB medium containing 0.1% dimethyl sulfoxide (Control), 50 µM LY294002 (LY294), 100 nM wortmannin (Wort), 10 µM ML-7, 20 µM ML-7 or 10 µM cytochalasin D (CyD). After 30-minute incubation at 4°C (for binding; white bars) or 37°C (for phagocytosis; black bars), the binding/phagocytic index (IgG-Es per cell) was scored as described in Materials and Methods. Bars show the mean and standard deviation of triplicate determinations (n=3) in a single experiment. Data are representative of at least three independent experiments.

suggesting that indirect inhibition of myosin II by the MLCK inhibitor perturbed FcR-mediated phagocytosis. The extent of inhibition by the myosin inhibitor was comparable to that of PI3K inhibitors. Thus, it seems likely that myosin II contributes to some aspect of FcR-mediated phagocytosis, although some other types of myosins might also be involved in phagocytosis. Cytochalasin D, an inhibitor of F-actin polymerization, completely inhibited phagocytosis, indicating the strict dependence of phagocytosis on F-actin polymerization (Fig. 1). All inhibitors did not significantly reduce the number of IgG-Es bound on the cell surface at 4°C (Fig. 1). This implies that these inhibitors affect the process of internalization of IgG-Es but not their binding ability.

To analyze the effects of these inhibitors on the mechanism of phagocytosis, we used fluorescence microscopy to examine the morphologies of IgG-Es and F-actin during phagocytosis. After 30 minutes with IgG-Es in the presence or absence of inhibitors, macrophages were fixed and incubated with FITC-conjugated anti-rabbit IgG (FITC–anti-IgG) to label extracellularly exposed IgG-Es, then with rhodamine-phalloidin to label F-actin. In control macrophages, IgG-Es were internalized into intracellular compartments and most F-actin was dissociated from the particle-adherent membranes. FITC–anti-IgG could not access the compartments containing IgG-Es, indicating that these compartments were closed phagosomes or phagolysosomes (Fig. 2A-C). In ML-7- or wortmannin-treated cells, however, IgG-Es remained associated with F-actin-rich structures, presumed phagocytic cups. Most of the IgG-Es associated with these cells were

Fig. 2. Phase-contrast and fluorescence microscopy of IgG-Es and F-actin during phagocytosis in macrophages treated with 0.1% dimethyl sulfoxide (control), 100 nM wortmannin or 10 µM ML-7. Macrophages were pretreated with one of the drugs for 15 minutes, fed IgG-Es and incubated for 30 minutes in the presence of the drug. After fixation, extracellularly exposed IgG-Es and F-actin were stained with FITC–anti-rabbit-IgG and rhodamine phalloidin, respectively. In control cells (A-C), IgG-Es were internalized in phagosomes and/or phagolysosomes, and were scarcely associated with F-actin. In wortmannin-treated cells (D-F), IgG-Es seemed to be surrounded by F-actin-rich protrusions but remained partially exposed to extracellular fluid. ML-7-treated macrophages (G-I) appeared similar to wortmannin-treated cells. (A,D,G) Phase-contrast images. (D,E,H) FITC images showing extracellular IgG-Es. (C,F,I) Rhodamine images showing F-actin. Bars, 10 µm.
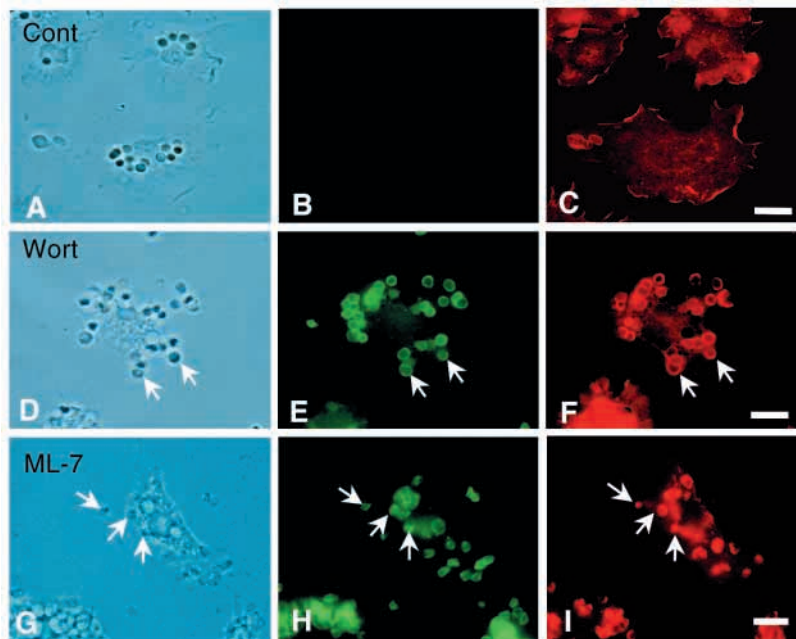
labeled with FITC, indicating that these IgG-Es surrounded by F-actin-rich protrusions were partially exposed to extracellular fluid (Fig. 2D-I). Differences between PI3K-inhibitor- and MLCK-inhibitor-treated cells were not evident under light microscopy. These data indicated that both PI3K inhibitors and MLCK inhibitor perturbed phagocytic-cup closure but not F-actin assembly for forming phagocytic cups. Unlike in PI3K-inhibitor- or MLCK-inhibitor-treated cells, F-actin assembly was not induced by the binding of IgG-Es in cytochalasin-D-treated cells. Consequently, neither phagocytic-cup formation nor internalized IgG-Es were observed in these cells (not shown).

Role for myosin in the phagocytic-cup squeezing

Consistent with light-microscopic observations, SEM revealed that, after 30 minutes, no IgG-Es were evident on the dorsal surface of control macrophages, indicating that IgG-Es were all intracellular (not shown). However,

cells fixed 7 minutes after adding IgG-Es showed phagocytic cups at various stages of formation. These cups engulfing IgG-Es frequently appeared cylindrical rather than spherical (Fig. 3A). In PI3K-inhibitor-treated cells, many IgG-Es were observed in phagocytic cups on the dorsal cell surface, because cup closure was arrested (Araki et al., 1996). The phagocytic cups formed in PI3K-inhibitor-treated cells were tightly fitted to the surface of IgG-Es and their distal margins remained open even at 30 minutes after beginning phagocytosis (Fig. 3B). The configurations of the phagocytic cups in PI3K-inhibited cells were similar to those observed in control cells fixed 7 minutes after addition of IgG-Es (Fig. 3A,B).

In ML-7-treated cells, phagocytic cups appeared to be somewhat shallower than those in PI3K-inhibitor-treated cells. Even though phagocytic cups formed around IgG-Es, the inner

Fig. 3. SEM of IgG-E phagocytosis in macrophages treated with the drugs. (A) A phagocytic cup in a control macrophage after 7-minute incubation with IgG-Es. The phagocytic cup is conformed closely to the surface of IgG-Es. The cylindrical cup appeared to have constricted the IgG-Es. After 30 minutes, IgG-Es were no longer seen on the cell surface, because all had been internalized by the cells (not shown). (B) In wortmannin-treated macrophages, many phagocytic cups were observed on the dorsal surface of macrophages. The configuration of phagocytic cups was similar to that in control cells at 7 minutes after phagocytosis. (C) ML-7 treatment also did not inhibit phagocytic-cup formation. Most strikingly, phagocytic cups were not closely apposed to the surfaces of IgG-Es. (D) Cytochalasin D inhibited phagocytic-cup formation. IgG-Es bound to the plane dorsal surface of the cells. Electron micrographs were pseudocolored using Adobe Photoshop. Bars, 5 µm.
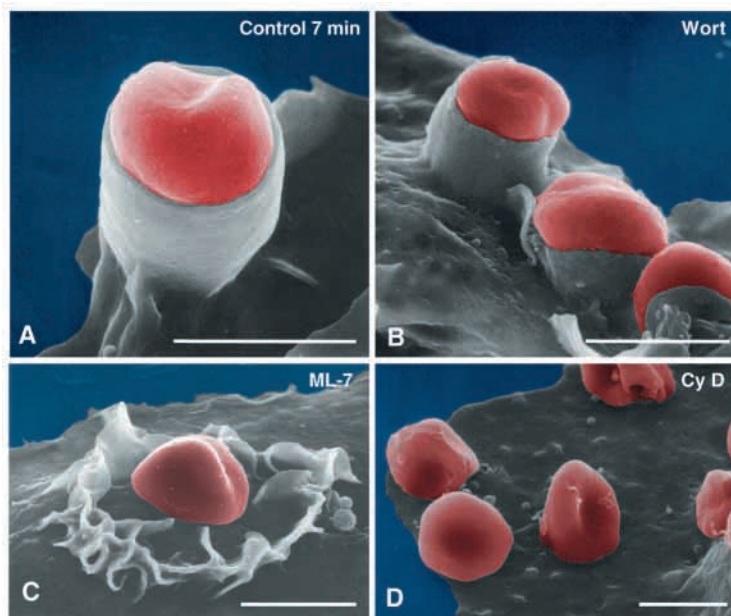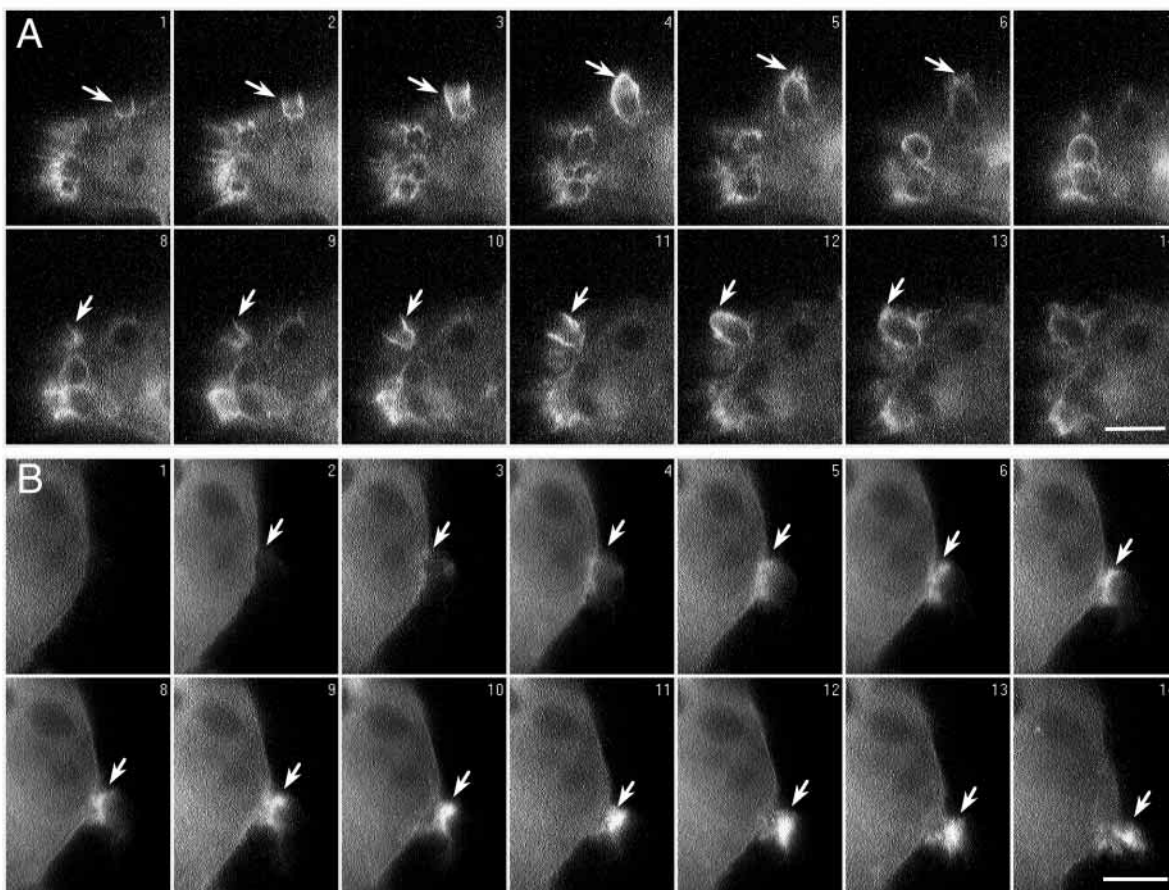
Fig. 4. Time-lapse sequences of living RAW264.1 macrophages transfected with pEGFP-actin, showing actin dynamics during phagocytosis of IgG-Es. (A) In a control cell, IgG-Es induced F-actin assembly where they were bound, resulting in phagocytic-cup formation. It was noteworthy that the IgG-Es was deformed during phagocytic-cup formation, suggesting that the F-actin ring constricted the phagocytic cup and squeezed the IgG-Es. Subsequently, the F-actin ring seemed to close at the top of the cup. F-actin disappeared immediately after phagocytic cups closed into intracellular phagosomes. (B) In a ML-7-treated cell, F-actin assembly and phagocytic-cup extension occurred, but the process was slower and the cup was shallower than in control. Even though phagocytic cups were formed, they did not constrict or close. The time interval between frames is 10 seconds. Bars, 10 μm. The supplemental video materials are available in the online version [Video 1 (http://www.jcs.biologists.org/supplemental)].

side face of phagocytic cups was not closely adherent to the surface of the IgG-Es, so phagocytic cups looked like flowers in bloom (Fig. 3C). This unique configuration of phagocytic cup indicated that cup side wall could extend without guidance from sequential IgG-FcR binding, and that myosin might be unnecessary for phagocytic cup formation but necessary for the close apposition of the cup side wall against opsonized particles. We scored the morphology of phagocytic cups in ML-7- and wortmannin-treated cells (100 of each). In wortmannin-treated cells, 82% of phagocytic cups apparently showed tight apposition to IgG-Es and others were loosely open or undefined. By contrast, in ML-7-treated cells, 45% of phagocytic cups were loosely open, 48% were short or irregular and only 7% were closely fitted against the IgG-Es. When F-actin polymerization was inhibited by cytochalasin-D treatment, IgG-Es bound to the dorsal cell surface but no phagocytic cup formation was evident (Fig. 3D). These SEM data also indicated that phagocytic cup side wall extension requires F-actin polymerization but not myosin II.

To explore further the actomyosin-driven constriction of phagocytic cups, we observed actin dynamics during phagocytosis in living RAW264.1 cells transfected with pEGFP-actin. Video microscopy of control cells showed that binding of IgG-Es induced GFP-actin accumulation underneath the plasma membrane near the particle. F-actin-enriched protrusions then extended along the surfaces of IgG-Es. In a side view of the phagocytic cup, a dense band of F-actin moved from the bottom toward the top of the phagocytic cup during extension. In a movie [Video 1A (http://www.jcs.biologists.org/supplemental)], it was notable that the IgG-Es in the phagocytic cup deformed along the axis of the phagocytic-cup extension, making it look like a deformable particle passing through a tight ring of F-actin. When the phagocytic cup was fully extended to enclose the particle, the F-actin band closed the top aperture of phagocytic cup to form an intracellular phagosome. Most F-actin then appeared to be immediately dissociated from the phagosomal membrane. The process of phagocytosis generally took 3-5 minutes from F-actin assembly to F-actin dissociation [Fig. 4A, Video 1A (http://www.jcs.biologists.org/supplemental)].

Phagocytic-cup extension also occurred in ML-7-treated cells but seemed to be somewhat slower than that in control cells. The phagocytic cups did not constrict or squeeze IgG-Es. Rather, they
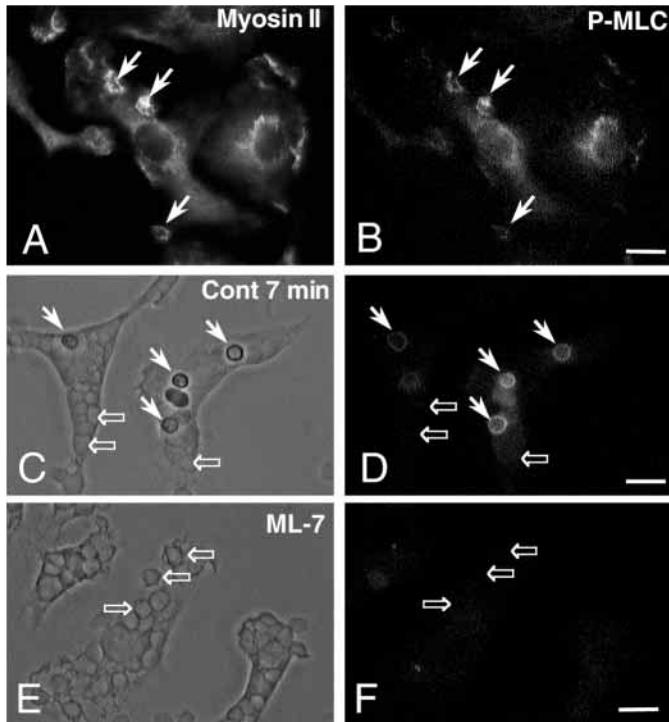
Fig. 5. Immunolocalization of myosin II and phosphorylated myosin light chain (P-MLC) in ruffles and phagocytic cups of macrophages. Immunofluorescence of myosin II (A) and P-MLC (B) in macrophages stimulated with M-CSF showed that MLC of myosin II are predominantly phosphorylated in cell-surface ruffles. (C,D) In control macrophages phagocytosing IgG-Es (7 minutes after feeding with IgG-Es), P-MLC localized in some phagocytic cups (arrows) but not in phagosomes (open arrows). (E,F) ML-7 treatment greatly reduced the amount of P-MLC in phagocytic cups. Phase-contrast images C and E correspond to fluorescence images D and F, respectively. Bars, 10 µm.
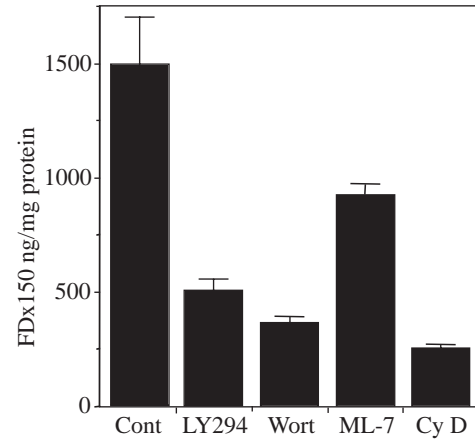

Fig. 6. Fluorometric quantitation of macropinocytosis. Macrophages were pretreated with 0.1% dimethyl sulfoxide (Control), 50 µM LY294002 (LY294), 100 nM wortmannin (Wort), 10 µM ML-7 or 10 µM cytochalasin D (CyD) for 15 minutes, and incubated with 1.0 mg ml^{-1} FDx150 in RB medium for 30 minutes to allow macropinocytosis. The fluorescence of cell lysates was assayed by spectrofluorometry. The values represent the mean plus or minus the standard deviation of triplicate determinations. Similar results were obtained in two additional experiments.

repeatedly elongated and shortened their side walls without closing into phagosomes. IgG-Es remained in unclosed phagocytic cups even at 30 minutes or more after IgG-E binding [Fig. 4B, Video 1B (http://www.jcs.biologists.org/supplemental)]. The effect of ML-7 on phagocytosis was reversible, because phagocytosis proceeded normally after washout of the drug (not shown). The cups formed in PI3K-inhibitor-treated cells did not close into phagosomes but they could deform IgG-Es during cup formation (not shown).

Next, we examined the localization of myosin II and phosphorylated myosin light chain (P-MLC) in macrophages. In macrophages stimulated with M-CSF, myosin II abundantly localized in active ruffles on the cell dorsal surface (Fig. 5A). Using an antibody specific to P-MLC, it was shown that myosin II light chain was phosphorylated in active ruffles (Fig. 5B). In control macrophages during phagocytosis, P-MLC was detected in some early stages of phagocytic cups (Fig. 5C,D). In ML-7-treated cells, P-MLC was scarcely seen in phagocytic cups, suggesting that ML-7 inhibited phosphorylation of MLC (Fig. 5E,F).

Role of myosin in macropinocytosis and ruffling

To analyze the myosin contribution to macropinocytosis, we first measured the effects of inhibitors for PI3K, MLCK and F-actin on pinocytosis of FDx150, a fluid-phase probe that is preferentially taken up by macropinocytosis (Araki et al., 1996; Araki and Swanson, 1998). Macropinocytosis was stimulated by the addition of M-CSF to the medium (Racoosin and Swanson, 1989). Cells were then incubated with 1 mg ml^{-1} FDx150 for 30 minutes in the absence or presence of inhibitors. Quantitative fluorometric analysis indicated that ML-7 significantly reduced intracellular accumulation of FDx150, although their inhibitory extent was somewhat less than that of PI3K inhibitors. Cytochalasin D perturbed fluid-phase pinocytosis of FDx150 most severely (Fig. 6). Even though the accumulation of FDx150 might be slightly influenced by F-actin-independent micropinocytosis, the comparative quantitation indicated that myosin II inhibition attenuated macropinocytosis. Similarly, fluorescence microscopy revealed that macropinosomes labeled with fixable FDx10 for 5 minutes were largely diminished by all of these inhibitors (not shown).

We next used time-lapse video microscopy to identify myosin-dependent activities associated with ruffling and macropinocytosis in living cells. Consistent with earlier observations (Araki et al., 1996), wortmannin-treated macrophages displayed dorsal surface ruffling and circular ruffle formation much like control cells. However, circular ruffles receded without closing into macropinosomes [Fig. 7A,B, Video 2A,B (http://www.jcs.biologists.org/supplemental)]. Unlike the PI3K inhibitors, however, MLCK inhibitor reduced most ruffle movement. In the ML-7-treated cells, the ruffles infrequently raised from the cell edge and showed a slow centripetal movement on the dorsal surface. Circular ruffle formation was not seen in MLCK-inhibited cells, indicating that such simple ruffling was insufficient for macropinocytosis [Fig. 7C, Video 2C (http://www.jcs.biologists.org/supplemental)]. Ruffling activity was quantified by digital image analysis of time-lapse phase-
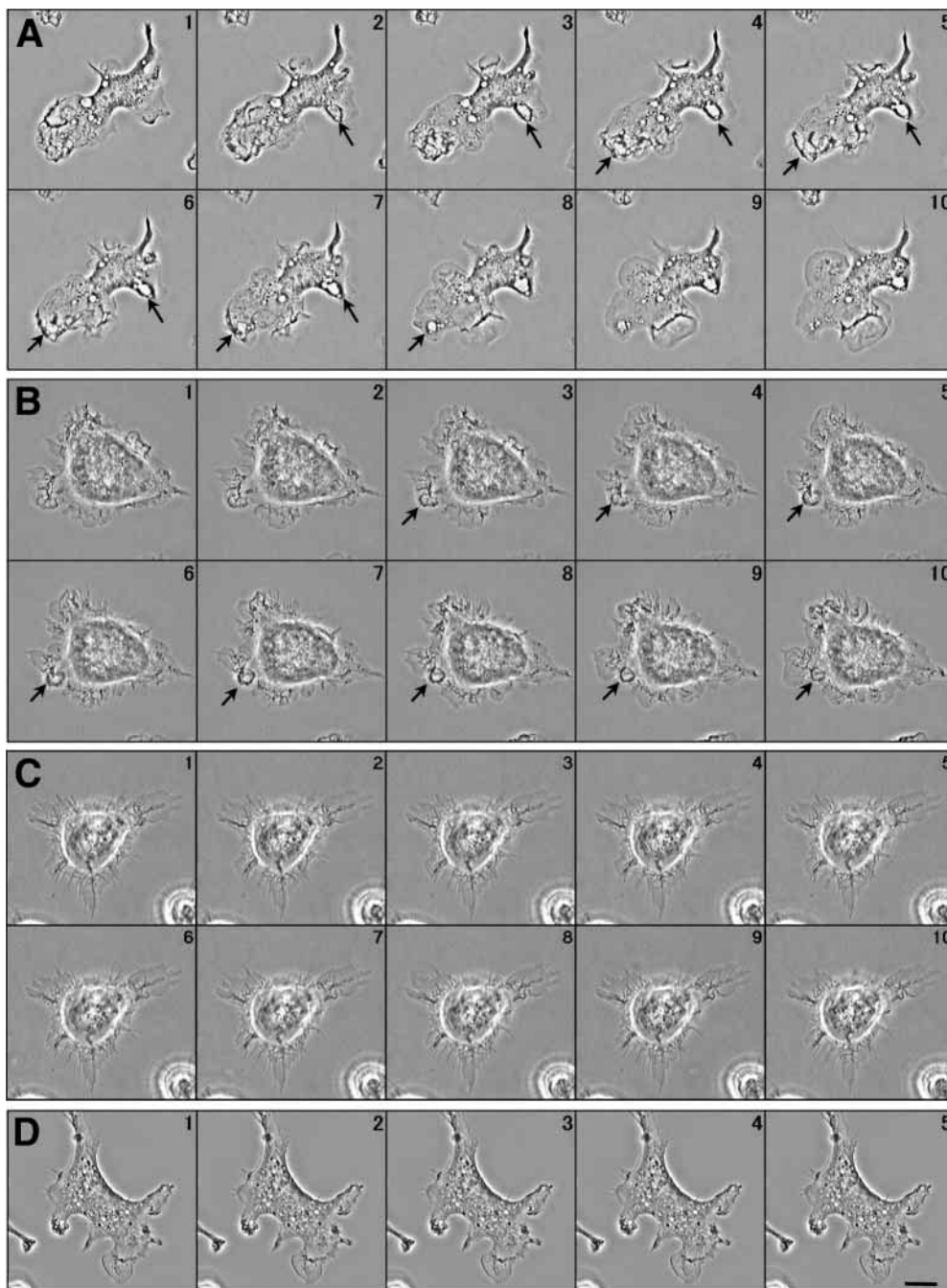
Fig. 7. Time-lapse sequences of ruffling and macropinocytosis. Macrophages were stimulated with 2000 U ml^{-1} M-CSF and treated with 0.1% dimethyl sulfoxide (control; A), 100 nM wortmannin (B), 10 μM ML-7 (C) or 10 μM cytochalasin D (D). Numbers indicate time sequence with 10-second intervals. Ruffles were seen as phase-dense bands in the periphery of the cells. (A) In control cells, phase-bright macropinosomes were formed by closing circular ruffles (arrows). (B) Wortmannin did not inhibit circular ruffle formation but did inhibit the closure of circular ruffles into macropinosomes (arrows). (C) In ML-7, ruffle movement was markedly reduced. No circular ruffle formation was observed. Only simple centripetal movement of ruffles was seen. (D) Cytochalasin D stopped the ruffle movement completely. Bar, 10 μm. The supplemental video materials are available in the online version [Video 2 (http://www.jcs.biologists.org/ supplemental)].

identified previously (Swanson et al., 1999).

In FcR-mediated phagocytosis, phagocytic-cup extension along the surface of IgG-opsonized particles has been explained by the 'zipper model', which implies sequential binding between cell surface FcR and Fc region of IgG on the particle surface (Greenberg and Silverstein, 1993). The interaction between IgG and FcR triggers the phosphorylation of specific tyrosine residues in the receptor within motifs termed ITAMs (immunoreceptor tyrosine-based activation motif) by the Src-family tyrosine kinases (Ghazizadeh et al., 1994; Greenberg et al., 1994; Cox et al., 1996; Cox et al., 1997; Crowley et al., 1997; Isakov, 1997). These early signals from ligated receptors lead to further signaling pathways involving lipid kinases, phospholipases and GTPases. (reviewed by Aderem and Underhill, 1999; Kwiatkowska and Sobota, 1999; Lennartz, 1999). Downstream, Rho-family members of monomeric GTPases such as Rac, Rho and Cdc42 induce F-actin polymerization and reorganization (Cox et al., 1997; Massol et al., 1998; Castellano et al., 2000; Chimini and Chavrier, 2000), changes which are also regulated by phosphoinositides such as PI(4,5)P$_2$ and PI(3,4,5)P$_3$ (Hackam et al., 1997; Botelho et al., 2000; Marshall et al., 2001). Many actin-binding proteins (e.g. actin-nucleating factors and F-actin bundling and severing

contrast images, which indicated that wortmannin or LY294002 reduced ruffling movements much less than ML-7-treatment did (Fig. 8, Table 1). These observations indicated that myosin II acts earlier than PI3K in the coordination of ruffling for macropinocytosis.

Discussion

This study demonstrates two distinct roles for myosin II in the mechanical processes of phagocytosis and macropinocytosis by macrophages: phagocytic cup squeezing and coordinated ruffling for circular ruffle formation. Because these contractile activities are evident in the presence of PI3K inhibitors, they are distinct from the PI3K-dependent contractile activities

Table 1. Digital quantitation of ruffling activity using subtracted images

Treatments	Ruffling indices±s.d. (n=10)
Control (M-CSF only)	45.83±3.30
50 µM LY294002	35.83±3.91
100 nM wortmannin	34.22±4.08
10 µM ML-7	22.33±2.08
10 µM cytochalasin D	10.12±1.83
Formaldehyde fixation	4.15±0.22

Each standard deviation of gray values in the cellular region of subtracted images (examples are shown in the subtracted images of Fig. 8) was scored from ten sequential subtracted images. The ruffling indices represent the average mean ± s.d. (n=10). The value of formaldehyde-fixed cell implies background noise. Similar results were obtained from two additional, independent experiments.

proteins) and myosins are involved in particle engulfment to form nascent phagosomes (Greenberg et al., 1990; Allen and Aderem, 1996b; Swanson et al., 1999; Titus, 1999; Araki et al., 2000; May et al., 2000). This complexity indicates that the zipper closure mechanism must be integrated by supplemental mechanisms. PI3K inhibition perturbs phagocytic-cup closure but not F-actin assembly or phagocytic-cup formation (Araki et al., 1996; Cox et al., 1999; Diakonova et al., 2002). Dynamin 2 recruitment to phagocytic cups is controlled by PI3K (Gold et al., 1999), although the function of dynamin in phagosome closure has not been determined. Furthermore, focal exocytosis of VAMP3-positive recycling vesicles to the site of particle uptake might be required for phagocytic-cup extension sufficient to enclose large particles (Banjo et al., 2000). Such full phagocytic-cup extension also depends on PI3K signaling (Cox et al., 1999).

To complete phagosome formation, some forces would be required for sequential binding and extension of phagocytic cups along particle surfaces. In neutrophils, regulation of phagocytosis by MLCK indicates that myosin II is involved in FcR-mediated phagocytosis of IgG-Es (Mansfield et al., 2000). Myosin II and MLCK contribute to many cell motilities such as lamellipodial movement and cytokinesis, and our quantitative measurements indicated that myosin II was required for FcR-mediated phagocytosis. Furthermore, our immunofluorescence localized P-MLC in phagocytic cups, and showed that phosphorylation of MLC in phagocytic cups was inhibited by ML-7. These immunolocalizations strongly supported the notion that myosin II plays an important role in the formation of phagosomes during FcR-mediated phagocytosis in macrophages. On the other hand, de Lanerolle et al. (de Lanerolle et al., 1993) reported that myosin phosphorylation did not significantly increase in J774 macrophages during phagocytosis of opsonized yeast; and electroinjection of anti-MLCK did not inhibited phagocytosis. However, they measured the total amount of phosphorylated myosin but not the net amount involved in FcR-mediated phagocytosis (de Lanerolle et al., 1993). Moreover, unlike IgG-Es, opsonized yeast would be phagocytosed by a nonopsonic, lectin-sugar (β-glucan and mannan) recognition mechanism even if FcR-mediated phagocytosis were inhibited (Le Cabec et al., 2000). It was also reported that *Dictyostelium* myosin-II-null mutant did not appear to have any defects in phagocytosis of living *Escherichia coli* (Maselli et al., 2002). This discrepancy might be due to differences in the cell types and/or the phagocytic targets. Some types of phagocytosis of nonopsonized particles or living bacteria might not require myosin II activity. Most recently, Olazabal et al. (Olazabal et al., 2002) showed that ML-7 also inhibited complement-receptor-mediated phagocytosis as well as actin recruitment to the site of phagocytosis. They further indicated that myosin II was required for FcR-mediated phagocytosis but not actin recruitment (Olazabal et al., 2002). Their findings on FcR-mediated phagocytosis were totally consistent with our data presented here. Therefore, myosin II and its phosphorylation seem to be required for FcR-mediated phagocytosis and complement-receptor-mediated phagocytosis. However, the role of myosin II might differ between the two types of phagocytosis, because they use different cytoskeletal components and signaling pathways during the engulfment of particles (Allen and Aderem, 1996b). Importantly, our
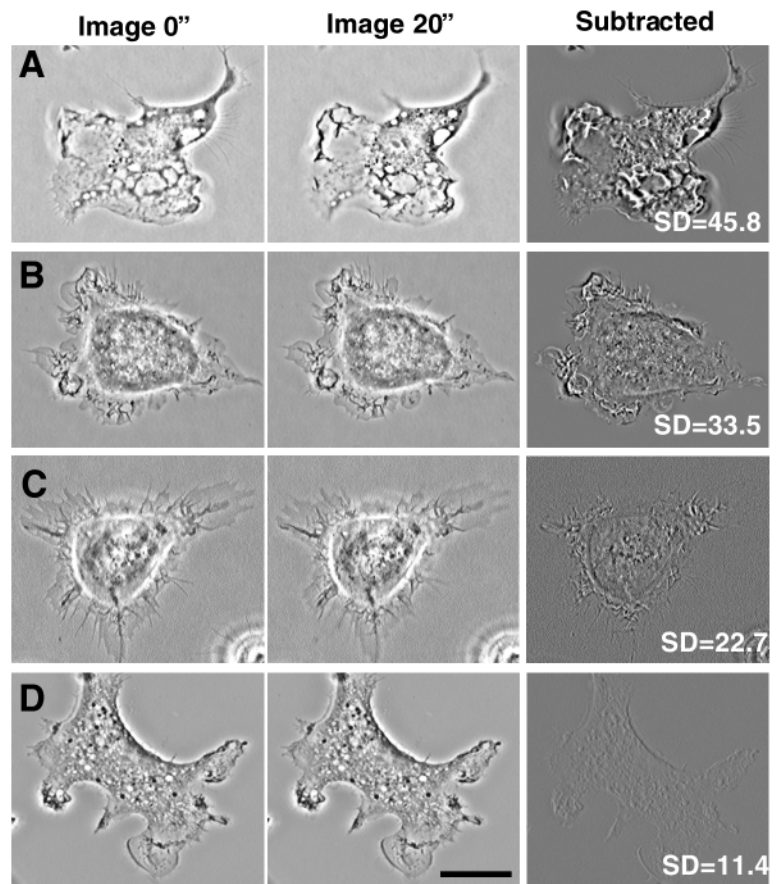

Fig. 8. Digital image analysis of ruffling activities in control (A), wortmannin-treated (B), ML-7-treated (C) and cytochalasin-D-treated cells (D). Subtracted images (right) were obtained by subtracting the images (center) from the frames taken 20 seconds earlier (left), then adding 120 to the gray value of each pixel. In subtracted images, the standard deviations (SD) of gray values of the cell area are shown. Bar, 10 µm.

morphological data now suggest a role for myosin II in phagocytic-cup squeezing during FcR-mediated phagocytosis.

Our SEM of control cells revealed that the side wall of phagocytic cups appeared tightly apposed to the IgG-Es and deformed IgG-Es in the phagocytic cups. This deformation of erythrocytes might be explained by a myosin-based contractile activity that squeezes particles during phagocytic cup formation. In ML-7-treated cells fed with IgG-Es, phagocytic cups were formed but remained unclosed, as in the PI3K inhibitor-treated cells. It was notable that, unlike PI3K-inhibited or normal phagocytic cups, their side walls were not closely apposed to the surface of particles. This unique configuration of bloomed flower-like phagocytic cups in MLCK-inhibited cells indicated, first, that phagocytic cup formation occurred without myosin activated by MLCK, and, second, that the sequential binding of FcR to IgG Fc was not required for phagocytic-cup extension. This free side wall extension of phagocytic cups might occur by directional actin polymerization pushing against plasma membrane (Theriot, 2000). Video microscopy of living cells transfected with pEGFP-actin indicated that an actin ring squeezed the phagocytic cup, resulting in deformation of the IgG-Es. ML-7 perturbed such squeezing activity without affecting actin polymerization at the site of IgG-E binding. This suggests that myosin II contributes to the squeezing, although other classes of myosins might also participate. In addition, upon myosin inhibition, phagocytic-cup extension was slowed and shortened, resulting in failure of phagocytic-cup closure. These findings indicate that myosin-II activity and sequential ligand-FcR binding co-operate to facilitate maximal phagocytic-cup extension for the engulfment of large particles. Such cooperative contractile activity might reinforce binding between the particle surface and the plasma membrane, particularly when the opsonization is weak. Moreover, because such squeezing would push extra-particle fluid out of phagosomes, this mechanism might decrease phagosomal volume and consequently increase lumenal concentrations of superoxide and protons needed for bacterial killing.

The phagocytic cups formed in myosin-inhibited cells resemble spacious phagosomes induced by bacteria such as *Salmonella typhimurium* (Alpuche-Aranda et al., 1994). In contrast to opsonized pathogens, which enter macrophages in tightly fitted phagosomes and are killed rapidly, these pathogens enter and survive inside phagosomes containing extracellular fluid. *S. typhimurium* might create spacious phagosomes by inhibiting the myosin-driven squeezing of the phagocytic cups. Alternatively, *S. typhimurium* might enter cells simply by inducing macropinocytosis locally. Other types of phagocytosis, besides FcR-mediated phagocytosis, show distinct characteristics in morphology, machineries and signaling (Rittig et al., 1999; Greenberg, 2001), and it would be of interest to elucidate the contributions of myosins to these processes.

In contrast to FcR-mediated phagocytosis, macropinocytosis efficiently engulfs extracellular fluid. Myosin II localized in active ruffles might be required to coordinate ruffling to form macropinosomes. Our video microscopic analysis indicated that M-CSF-stimulated ruffling was much reduced by ML-7, but was not much affected by PI3K inhibitors. Upon inhibition of MLCK, ruffle movements became much slower than those observed in control cells, and circular ruffles did not form. These findings suggest that myosin II is required for circular ruffle formation, which can be regarded as the initial process of macropinocytosis. However, myosin-based motility in macropinocytosis is likely to be highly complex, involving different isoforms and classes of myosins that perform distinct functions. Other classes of myosins appear to participate in later stages of macropinocytosis than circular ruffle formation. For instance, *Dictyostelium* myosin-I-knockout strains show increased circular ruffles, probably because of defects in later stages of macropinocytosis (Novak et al., 1995; Jung et al., 1996). Perhaps myosin I contributes to macropinosome closure in macropinocytosis, similar to the phagocytic-cup closure in phagocytosis.

Because PI3K inhibitors attenuated both phagocytosis and macropinocytosis at later stages than the MLCK inhibitor did, we infer that the relevant myosin-II activity is independent of PI3K. Other signaling pathways than the PI3K cascade might modulate myosin-II function. Rac1 and Cdc42 are implicated in the actin cytoskeleton remodeling during phagocytosis and macropinocytosis (Ridley et al., 1992; Cox et al., 1997; Massol et al., 1998; Dumontier et al., 2000; Nobes and Marsh, 2000), and p21-activated kinase 1 (PAK1), which is a direct target for Rac1 and Cdc42, is located in phagocytic cups and circular ruffles (Dharmawardhane et al., 1999). Moreover, a constitutively active PAK1 mutant induced the formation of circular ruffles (Dharmawardhane et al., 1997). Interestingly, PAK1 affects the phosphorylation state of MLC and eventually regulates cell movements by myosin II (Sells et al., 1999). These observations, together with the fact that actin–myosin-II interactions are regulated by the phosphorylation of MLC (Somlyo and Somlyo, 1994), indicate that myosin II participates in Rac1 and Cdc42-induced cellular movements for FcR-mediated phagocytosis and macropinocytosis. It is likely that Ca^{2+} is also required for FcR-mediated phagocytosis, because MLCK activity depends on Ca^{2+}/calmodulin (Saitoh et al., 1987). Although it is known that FcR ligation is accompanied by rises in cytosolic free Ca^{2+} concentration, the requirement for Ca^{2+} in FcR-mediated phagocytosis is still controversial (Edberg et al., 1995; Hackam et al., 1997; Greenberg, 2001). Further studies will be needed to clarify the role of Ca^{2+} in phagocytosis and macropinocytosis.

The PI3K-independent activity described here is distinct from the PI3K-dependent contractile activities described previously (Araki et al., 1996; Swanson et al., 1999). Myosins I or X might close circular ruffles and phagocytic cups in a PI3K-dependent manner. It is conceivable that the binding of myosin I to plasma membrane is regulated by phosphoinositides such as $PI(3,4)P_2$ and $PI(3,4,5)P_3$ (Adams and Pollard, 1989; Zhou et al., 1998). Moreover, myosin X contains a pleckstrin-homology domain that recognizes $PI(3,4,5)P_3$ (Berg et al., 2000). Cox et al. (Cox et al., 2002) have shown that myosin X localizes phagosomes in a wortmannin-sensitive manner. These results are consistent with myosins IC or X serving as the PI3K-dependent contractile proteins that close phagosomes. In conclusion, we now distinguish three component activities of the actin cytoskeleton during phagocytosis and macropinocytosis. (1) Stimulated actin polymerization for phagocytic cup extension. (2) PI3K-independent, myosin-II-dependent contractile activities that

squeeze phagocytic cups and curve ruffles. (3) PI3K-dependent contractile activities that constrict the distal margins of cup-shaped protrusions and complete phagosome/macropinosome closure.

References

Adams, R. J. and Pollard, T. D. (1989). Binding of myosin I to membrane lipids. *Nature* **340**, 565-568.

Aderem, A. and Underhill, D. M. (1999). Mechanisms of phagocytosis in macrophages. *Annu. Rev. Immunol.* **17**, 593-623.

Al-Haddad, A., Shonn, M. A., Redlich, B., Blocker, A., Burkhardt, J. K., Yu, H., Hammer, J. A., 3rd, Weiss, D. G., Steffen, W., Griffiths, G. et al. (2001). Myosin Va bound to phagosomes binds to F-actin and delays microtubule-dependent motility. *Mol. Biol. Cell* **12**, 2742-2755.

Allen, L. A. and Aderem, A. (1996a). Mechanisms of phagocytosis. *Curr. Opin. Immunol.* **8**, 36-40.

Allen, L. A. and Aderem, A. (1996b). Molecular definition of distinct cytoskeletal structures involved in complement- and Fc receptor-mediated phagocytosis in macrophages. *J. Exp. Med.* **184**, 627-637.

Allen, L. H. and Aderem, A. (1995). A role for MARCKS, the alpha isozyme of protein kinase C and myosin I in zymosan phagocytosis by macrophages. *J. Exp. Med.* **182**, 829-840.

Alpuche-Aranda, C. M., Racoosin, E. L., Swanson, J. A. and Miller, S. I. (1994). *Salmonella* stimulate macrophage macropinocytosis and persist within spacious phagosomes. *J. Exp. Med.* **179**, 601-608.

Araki, N., Hatae, T., Yamada, T. and Hirohashi, S. (2000). Actinin-4 is preferentially involved in circular ruffling and macropinocytosis in mouse macrophages: analysis by fluorescence ratio imaging. *J. Cell Sci.* **113**, 3329-3340.

Araki, N., Johnson, M. T. and Swanson, J. A. (1996). A role for phosphoinositide 3-kinase in the completion of macropinocytosis and phagocytosis by macrophages. *J. Cell Biol.* **135**, 1249-1260.

Araki, N. and Swanson, J. A. (1998). Labeling of endocytic vesicles using fluorescent probes for fluid-phase endocytosis. In *Cell Biology: A Laboratory Handbook*, Vol. 2 (ed. J. E. Celis), pp. 495-500. San Diego: Academic Press.

Banjo, L., Peng, X.-R., Schreiber, A. D., Moore, H.-P., Trimble, W. S. and Grinstein, S. (2000). Focal exocytosis of VAMP3-containing vesicles at sites of phagosome formation. *J. Cell Biol.* **149**, 697-705.

Berg, J. S., Derfler, B. H., Pennisi, C. M., Corey, D. P. and Cheney, R. E. (2000). Myosin-X, a novel myosin with pleckstrin homology domains, associates with regions of dynamic actin. *J. Cell Sci.* **113**, 3439-3451.

Botelho, R. J., Teruel, M., Dierckman, R., Anderson, R., Wells, A., York, J. D., Meyer, T. and Grinstein, S. (2000). Localized biphasic changes in phosphatidylinositol-4,5-bisphosphate at sites of phagocytosis. *J. Cell Biol.* **151**, 1353-1368.

Castellano, F., Montcourrier, P. and Chavrier, P. (2000). Membrane recruitment of Rac1 triggers phagocytosis. *J. Cell Sci.* **113**, 2955-2961.

Chimini, G. and Chavrier, P. (2000). Function of Rho family proteins in actin dynamics during phagocytosis and engulfment. *Nat. Cell Biol.* **2**, E191-E196.

Cox, D., Chang, P., Kurosaki, T. and Greenberg, S. (1996). Syk tyrosine kinase is required for immunoreceptor tyrosine activation motif-dependent actin assembly. *J. Biol. Chem.* **271**, 16597-16602.

Cox, D., Chang, P., Zhang, Q., Reddy, P. G., Bokoch, G. M. and Greenberg, S. (1997). Requirements for both Rac1 and Cdc42 in membrane ruffling and phagocytosis in leukocytes. *J. Exp. Med.* **186**, 1487-1494.

Cox, D., Tseng, C. C., Bjekic, G. and Greenberg, S. (1999). A requirement for phosphatidylinositol 3-kinase in pseudopod extension. *J. Biol. Chem.* **274**, 1240-1247.

Cox, D., Berg, J. S., Cammer, M., Chinegwundoh, J. O., Dale, B. M., Cheney, R. E. and Greenberg, S. (2002). Myosin-X is a downstream effector of PI(3)K during phagocytosis. *Nat. Cell Biol.* **4**, 469-477.

Crowley, M. T., Costello, P. S., Fitzer-Attas, C. J., Turner, M., Meng, F., Lowell, C., Tybulewicz, V. L. and DeFranco, A. L. (1997). A critical role for Syk in signal transduction and phagocytosis mediated by Fcgamma receptors on macrophages. *J. Exp. Med.* **186**, 1027-1039.

de Lanerolle, P., Gorgas, G., Li, X. and Schluns, K. (1993). Myosin light chain phosphorylation does not increase during yeast phagocytosis by macrophages. *J. Biol. Chem.* **268**, 16883-16886.

Dharmawardhane, S., Sanders, L. C., Martin, S. S., Daniels, R. H. and Bokoch, G. M. (1997). Localization of p21-activated kinase 1 (PAK1) to pinocytic vesicles and cortical actin structures in stimulated cells. *J. Cell Biol.* **138**, 1265-1278.

Dharmawardhane, S., Brownson, D., Lennartz, M. and Bokoch, G. M. (1999). Localization of p21-activated kinase 1 (PAK1) to pseudopodia, membrane ruffles, and phagocytic cups in activated human neutrophils. *J. Leukocyte Biol.* **66**, 521-527.

Diakonova, M., Bokoch, G. and Swanson, J. A. (2002). Dynamics of cytoskeletal proteins during Fcγ receptor-mediated phagocytosis in macrophages. *Mol. Biol. Cell* **13**, 402-411.

Didichenko, S. A., Segal, A. W. and Thelen, M. (2000). Evidence for a pool of coronin in mammalian cells that is sensitive to PI 3-kinase. *FEBS Lett.* **485**, 147-152.

Dumontier, M., Hocht, P., Mintert, U. and Faix, J. (2000). Rac1 GTPases control filopodia formation, cell motility, endocytosis, cytokinesis and development in *Dictyostelium*. *J. Cell Sci.* **113**, 2253-2265.

Edberg, J. C., Lin, C. T., Lau, D., Unkeless, J. C. and Kimberly, R. P. (1995). The Ca^{2+} dependence of human Fc gamma receptor-initiated phagocytosis. *J. Biol. Chem.* **270**, 22301-22307.

Ghazizadeh, S., Bolen, J. B. and Fleit, H. B. (1994). Physical and functional association of Src-related protein tyrosine kinases with Fc gamma RII in monocytic THP-1 cells. *J. Biol. Chem.* **269**, 8878-8884.

Gold, E. S., Underhill, D. M., Morrissette, N. S., Guo, J., McNiven, M. A. and Aderem, A. (1999). Dynamin 2 is required for phagocytosis in macrophages. *J. Exp. Med.* **190**, 1849-1856.

Greenberg, S. (2001). Diversity in phagocytic signaling. *J. Cell Sci.* **114**, 1039-1040.

Greenberg, S., Burridge, K. and Silverstein, S. C. (1990). Colocalization of F-actin and talin during Fc receptor-mediated phagoctosis in mouse macrophages. *J. Exp. Med.* **172**, 1853-1856.

Greenberg, S., Chang, P. and Silverstein, S. C. (1994). Tyrosine phosphorylation of the gamma subunit of Fc gamma receptors, p72syk, and paxillin during Fc receptor-mediated phagocytosis in macrophages. *J. Biol. Chem.* **269**, 3897-3902.

Greenberg, S. and Silverstein, S. C. (1993). Phagocytosis. In *Fundamental Immunology*, 3rd edn (ed. W. E. Paul), pp. 941-964. New York: Raven Press.

Hackam, D. J., Rotstein, O. D., Schreiber, A., Zhang, W. and Grinstein, S. (1997). Rho is required for the initiation of calcium signaling and phagocytosis by Fcgamma receptors in macrophages. *J. Exp. Med.* **186**, 955-966.

Isakov, N. (1997). Immunoreceptor tyrosine-based activation motif (ITAM), a unique module linking antigen and Fc receptors to their signaling cascades. *J. Leukocyte Biol.* **61**, 6-16.

Jung, G., Wu, X. and Hammer, J. A., 3rd (1996). *Dictyostelium* mutants lacking multiple classic myosin I isoforms reveal combinations of shared and distinct functions. *J. Cell Biol.* **133**, 305-323.

Kwiatkowska, K. and Sobota, A. (1999). Signaling pathways in phagocytosis. *BioEssays* **21**, 422-431.

Le Cabec, V., Cols, C. and Maridonneau-Parini, I. (2000). Nonopsonic phagocytosis of zymosan and *Mycobacterium kansasii* by CR3 (CD11b/CD18) involves distinct molecular determinants and is or is not coupled with NADPH oxidase activation. *Infect. Immun.* **68**, 4736-4745.

Lennartz, M. R. (1999). Phospholipases and phagocytosis: the role of phospholipid-derived second messengers in phagocytosis. *Int. J. Biochem. Cell Biol.* **31**, 415-430.

Mansfield, P. J., Shayman, J. A. and Boxer, L. A. (2000). Regulation of polymorphonuclear leukocyte phagocytosis by myosin light chain kinase after activation of mitogen-activated protein kinase. *Blood* **95**, 2407-2412.

Marshall, J. G., Booth, J. W., Stambolic, V., Mak, T., Balla, T., Schreiber, A. D., Meyer, T. and Grinstein, S. (2001). Restricted accumulation of phosphatidylinositol 3-kinase products in a plasmalemmal subdomain during Fcγ receptor-mediated phagocytosis. *J. Cell Biol.* **153**, 1369-1380.

Maselli, A., Laevsky, G. and Knecht, D. A. (2002). Kinetics of binding, uptake and degradation of live fluorescent (DsRed) bacteria by *Dictyostelium discoideum*. *Microbiology* **148**, 413-420.

Massol, P., Montcourrier, P., Guillemot, J. C. and Chavrier, P. (1998). Fc receptor-mediated phagocytosis requires CDC42 and Rac1. *EMBO J.* **17**, 6219-6229.

May, R. C., Caron, E., Hall, A. and Machesky, L. M. (2000). Involvement

of Arp2/3 complex in phagocytosis mediated by FcγR or CR3. *Nat. Cell Biol.* **2**, 246-248.

May, R. C. and Machesky, L. M. (2001). Phagocytosis and the actin cytoskeleton. *J. Cell Sci.* **114**, 1061-1077.

Niewohner, J., Weber, I., Maniak, M., Muller-Taubenberger, A. and Gerisch, G. (1997). Talin-null cells of *Dictyostelium* are strongly defective in adhesion to particle and substrate surfaces and slightly impaired in cytokinesis. *J. Cell Biol.* **138**, 349-361.

Nobes, C. and Marsh, M. (2000). Dendritic cells: new roles for Cdc42 and Rac in antigen uptake? *Curr. Biol.* **10**, R739-R741.

Norbury, C. C., Hewlett, L. J., Prescott, A. R., Shastri, N. and Watts, C. (1995). Class I MHC presentation of exogenous soluble antigen via macropinocytosis in bone marrow macrophages. *Immunity* **3**, 783-791.

Novak, K. D., Peterson, M. D., Reedy, M. C. and Titus, M. A. (1995). *Dictyostelium* myosin I double mutants exhibit conditional defects in pinocytosis. *J. Cell Biol.* **131**, 1205-1221.

Olazabal, I. M., Caron, E., May, R. C., Schilling, K., Knecht, D. A. and Machesky, L. M. (2002). Rho-kinase and myosin-II control phagocytic cup formation during CR, but not FcγR, phagocytosis. *Curr. Biol.* **12**, 1413-1418.

Racoosin, E. L. and Swanson, J. A. (1989). Macrophage colony-stimulating factor (rM-CSF) stimulates pinocytosis in bone marrow-derived macrophages. *J. Exp. Med.* **170**, 1635-1648.

Racoosin, E. L. and Swanson, J. A. (1992). M-CSF-induced macropinocytosis increases solute endocytosis but not receptor-mediated endocytosis in mouse macrophages. *J. Cell Sci.* **102**, 867-880.

Radhakrishna, H., Klausner, R. D. and Donaldson, J. G. (1996). Aluminum fluoride stimulates surface protrusions in cells overexpressing the ARF6 GTPase. *J. Cell Biol.* **134**, 935-947.

Ridley, A. J., Paterson, H. F., Johnston, C. L., Diekmann, D. and Hall, A. (1992). The small GTP-binding protein Rac regulates growth factor-induced membrane ruffling. *Cell* **70**, 401-410.

Rittig, M. G., Wilske, B. and Krause, A. (1999). Phagocytosis of microorganisms by means of overshooting pseudopods: where do we stand? *Microbes Infect.* **1**, 727-735.

Ruchhoeft, M. L. and Harris, W. A. (1997). Myosin functions in *Xenopus* retinal ganglion cell growth cone motility *in vivo*. *J. Neurobiol.* **32**, 567-578.

Saitoh, M., Ishikawa, T., Matsushima, S., Naka, M. and Hidaka, H. (1987). Selective inhibition of catalytic activity of smooth muscle myosin light chain kinase. *J. Biol. Chem.* **262**, 7796-7801.

Sallusto, F., Cella, M., Danieli, C. and Lanzavecchia, A. (1995). Dendritic cells use macropinocytosis and the mannose receptor to concentrate macromolecules in the major histocompatibility complex class II compartment: downregulation by cytokines and bacterial products. *J. Exp. Med.* **182**, 389-400.

Sells, M. A., Boyd, J. T. and Chernoff, J. (1999). p21-activated kinase 1 (Pak1) regulates cell motility in mammalian fibroblasts. *J. Cell Biol.* **145**, 837-849.

Somlyo, A. P. and Somlyo, A. V. (1994). Signal transduction and regulation in smooth muscle. *Nature* **372**, 231-236.

Stendahl, O. I., Hartwig, J. H., Brotschi, E. A. and Stossel, T. P. (1980). Distribution of actin-binding protein and myosin in macrophages during spreading and phagocytosis. *J. Cell Biol.* **84**, 215-224.

Swanson, J. A. and Baer, S. C. (1995). Phagocytosis by zippers and triggers. *Trends Cell Biol.* **5**, 89-93.

Swanson, J. A. and Watts, C. (1995). Macropinocytosis. *Trends Cell Biol.* **5**, 424-428.

Swanson, J. A., Johnson, M. T., Beningo, K., Post, P., Mooseker, M. and Araki, N. (1999). A contractile activity that closes phagosomes in macrophages. *J. Cell Sci.* **112**, 307-316.

Theriot, J. A. (2000). The polymerization motor. *Traffic* **1**, 19-28.

Titus, M. A. (1999). A class VII unconventional myosin is required for phagocytosis. *Curr. Biol.* **9**, 1297-1303.

Vieira, O. V., Botelho, R. J., Rameh, L., Brachmann, S. M., Matsuo, T., Davidson, H. W., Schreiber, A., Backer, J. M., Cantley, L. C. and Grinstein, S. (2001). Distinct roles of class I and class III phosphatidylinositol 3-kinase in phagosome formation and maturation. *J. Cell Biol.* **155**, 19-25.

West, M. A., Prescott, A. R., Eskelinen, E. L., Ridley, A. J. and Watts, C. (2000). Rac is required for constitutive macropinocytosis by dendritic cells but does not control its downregulation. *Curr. Biol.* **10**, 839-848.

Zhang, Q., Calafat, J., Janssen, H. and Greenberg, S. (1999). ARF6 is required for growth factor- and Rac-mediated membrane ruffling in macrophages at a stage distal to Rac membrane targeting. *Mol. Cell. Biol.* **19**, 8158-8168.

Zhou, K., Pandol, S., Bokoch, G. and Traynor-Kaplan, A. E. (1998). Disruption of *Dictyostelium* PI3K genes reduces [^{32}P]phosphatidylinositol 3,4 bisphosphate and [^{32}P]phosphatidylinositol trisphosphate levels, alters F-actin distribution and impairs pinocytosis. *J. Cell Sci.* **111**, 283-294.